Published for SISSA by Springer

Received: *June 20, 2013*
Accepted: *August 7, 2013*
Published: *September 10, 2013*

Measurement of charm fragmentation fractions in photoproduction at HERA

The ZEUS collaboration

E-mail: levy@alzt.tau.ac.il

Abstract: The production of D^0, D^{*+}, D^+, D_s^+ and Λ_c^+ charm hadrons and their antiparticles in ep scattering at HERA has been studied with the ZEUS detector, using a total integrated luminosity of 372 pb^{-1}. The fractions of charm quarks hadronising into a particular charm hadron were derived. In addition, the ratio of neutral to charged D-meson production rates, the fraction of charged D mesons produced in a vector state, and the stangeness-suppression factor have been determined. The measurements have been performed in the photoproduction regime. The charm hadrons were reconstructed in the range of transverse momentum $p_T > 3.8\,\text{GeV}$ and pseudorapidity $|\eta| < 1.6$. The charm fragmentation fractions are compared to previous results from HERA and from e^+e^- experiments. The data support the hypothesis that fragmentation is independent of the production process.

Keywords: Lepton-Nucleon Scattering, QCD, Charm physics

Open Access

doi:10.1007/JHEP09(2013)058

JHEP09(2013)058

Contents

JHEP09(2013)058

1 Introduction

The fragmentation fractions of charm quarks into specific charm hadrons cannot be predicted by Quantum Chromodynamics (QCD) and have to be measured. It is usually assumed that they are universal, i.e. the same for charm quarks produced in e^+e^- annihilation, in ep collisions and also in pp or other hadronic collisions, even though the charm production mechanisms are not the same: in e^+e^- collisions, $c\bar{c}$ pairs are produced dominantly by QED pair production, whereas in ep collisions, the main production mechanism is the QCD boson-gluon fusion process $\gamma g \to c\bar{c}$. The fragmentation universality can be tested by measuring the fragmentation fractions at HERA and comparing the results with those obtained with e^+e^- collisions. Additionally, the values of the fragmentation fractions are crucial parameters used in comparisons of perturbative QCD (pQCD) calculations with measurements of charm production at HERA and elsewhere.

In this paper, measurements of the photoproduction of charm hadrons in ep collisions at HERA are presented. The relative production rates of the most copiously produced charm ground states, the D^0, D^+, D_s^+ mesons and the Λ_c baryon, and of the D^{*+} meson were measured.[1] The fractions of charm quarks hadronising into a particular charm hadron, $f(c \to D, D^*, \Lambda_c)$ were determined in the kinematic range of transverse momentum $p_T(D, D^*, \Lambda_c) > 3.8\,\text{GeV}$ and pseudorapidity $|\eta(D, D^*, \Lambda_c)| < 1.6$ of the charm state. Here D stands for D^0, D^+ and D_s^+ mesons. In addition, the ratio of neutral to charged D-meson production rates, the fraction of charged D mesons produced in a vector state, and the strangeness-suppression factor were determined.

The analysis presented here is based on an independent data set with an integrated luminosity over 4.5 times larger than the previous ZEUS measurement [1]. The new measurement benefits also from the ZEUS microvertex detector (MVD), which made it possible to identify the secondary decay vertices of the charm ground states and thereby to suppress background significantly. The new results are compared to the previous ZEUS measurement [1] in photoproduction, other HERA results from H1 [2] and ZEUS [3, 4] in deep inelastic scattering, and to results from experiments at the e^+e^- storage rings CLEO [5, 6], ARGUS [7–9] and the LEP experiments [10–15]. A summary is given in [16], with an update to 2010 branching ratios [17].

2 Experimental set-up

The analysis was performed with data taken from 2004 to 2007, when HERA collided electrons or positrons with energy $E_e = 27.5$ GeV and protons with energy $E_p = 920$ GeV. The corresponding total integrated luminosity was $372 \pm 7\ \text{pb}^{-1}$.

A detailed description of the ZEUS detector can be found elsewhere [18]. A brief outline of the components that are most relevant for this analysis is given below.

In the kinematic range of the analysis, charged particles were tracked in the central tracking detector (CTD) [19–21] and the microvertex detector (MVD) [22]. These components operated in a magnetic field of 1.43 T provided by a thin superconducting solenoid. The CTD consisted of 72 cylindrical drift-chamber layers, organised in nine superlayers covering the polar-angle[2] region $15° < \theta < 164°$. The MVD silicon tracker consisted of a barrel (BMVD) and a forward (FMVD) section. The BMVD contained three layers and provided polar-angle coverage for tracks from 30° to 150°. The four-layer FMVD extended the polar-angle coverage in the forward region to 7°. After alignment, the single-hit resolution of the MVD was 24 μm. The transverse distance of closest approach (DCA) of tracks to the nominal vertex in XY was measured to have a resolution, averaged over the azimuthal angle, of $(46 \oplus 122/p_T)$ μm, with p_T in GeV. For CTD-MVD tracks that pass through all nine CTD superlayers, the momentum resolution was $\sigma(p_T)/p_T = 0.0029 p_T \oplus 0.0081 \oplus 0.0012/p_T$, with p_T in GeV.

[1] For all studied charm hadrons, the charge conjugated states are implied throughout the paper.

[2] The ZEUS coordinate system is a right-handed Cartesian system, with the Z axis pointing in the nominal proton beam direction, referred to as the "forward direction", and the X axis pointing left towards the centre of HERA. The coordinate origin is at the centre of the CTD. The pseudorapidity is defined as $\eta = -\ln\left(\tan\frac{\theta}{2}\right)$, where the polar angle, θ, is measured with respect to the Z axis.

JHEP09(2013)058

The high-resolution uranium-scintillator calorimeter (CAL) [23–26] consisted of three parts: the forward (FCAL), the barrel (BCAL) and the rear (RCAL) calorimeters. Each part was subdivided transversely into towers and longitudinally into one electromagnetic section (EMC) and either one (in RCAL) or two (in BCAL and FCAL) hadronic sections (HAC). The smallest subdivision of the calorimeter was called a cell. The CAL energy resolutions, as measured under test-beam conditions, were $\sigma(E)/E = 0.18/\sqrt{E}$ for electrons and $\sigma(E)/E = 0.35/\sqrt{E}$ for hadrons, with E in GeV.

The luminosity was measured using the Bethe-Heitler reaction $ep \to e\gamma p$ by a luminosity detector which consisted of independent lead-scintillator calorimeter [27–29] and magnetic-spectrometer [30] systems. The fractional systematic uncertainty on the measured luminosity was 1.9 %.

3 Monte Carlo simulation

Monte Carlo (MC) simulations were used in the analysis for modelling signal and background processes and to correct the data for acceptance effects. MC samples of charm and beauty photoproduction events were produced with the Pythia 6.416 event generator [31]. The generation of events, based on leading-order matrix elements, includes direct photon processes, in which the photon couples as a point-like object in the hard scatter, and resolved photon processes, where the photon acts as a source of partons, one of which participates in the hard scattering process. Initial- and final-state parton showering is added to simulate higher-order processes. The CTEQ5L [32] and GRV LO [33] parametrisations were used for the parton distribution functions of the proton and photon, respectively. The charm (beauty) quark masses were set to 1.5 (4.75) GeV. Events for all processes were generated in proportion to the predicted MC cross sections. The Lund string model [34] as implemented in Jetset [31] was used for hadronisation in Pythia. The Bowler modification [35] of the Lund symmetric fragmentation function [36] was used for the longitudinal component of the charm- and beauty-quark fragmentation. The generated events were passed through a full simulation of the detector using Geant 3.21 [37] and processed with the same reconstruction program as used for the data.

To ensure a good description of the data, a reweighting was applied to the transverse momentum, $p_T(D, D^*, \Lambda_c)$, and pseudorapidity, $\eta(D, D^*, \Lambda_c)$, distributions of the Pythia MC samples. The reweighting factors were tuned using a large D^{*+} sample. The factors deviate by no more than $\pm 15\%$ from unity. The effect of the reweighting on the measured fragmentation fractions was small; the reweighting uncertainty was included in the systematic uncertainty.

4 Event selection

A three-level trigger system [38] was used to select events online. The first- and second-level trigger used CAL and CTD data to select ep collisions and to reject beam-gas events. At the third level, the full event information was available. The sample used in this analysis

JHEP09(2013)058

was mainly selected by third-level triggers where at least one reconstructed charm-hadron candidate was required. A dijet trigger was used in addition to increase the efficiency.

Photoproduction events were selected by requiring that no scattered electron with energy of greater than 5 GeV be identified in the CAL [39]. The photon-proton centre-of-mass energy, W, was reconstructed using the Jacquet-Blondel [40] estimator of W, $W_{\mathrm{JB}} = \sqrt{2E_p \sum_i E_i(1-\cos\theta_i)}$. Here E_i and θ_i denote the energy and polar angle of the i^{th} energy-flow object (EFO) [41], respectively, and the sum i runs over all final-state energy-flow objects built from CTD-MVD tracks and energy clusters measured in the CAL. After correcting for detector effects, the most important of which were energy losses in inactive material in front of the CAL and particle interactions in the beam pipe [39, 42], events were selected in the interval $130 < W_{\mathrm{JB}} < 300$ GeV. The lower limit was set by the trigger requirements, while the upper limit was imposed to suppress remaining DIS events with an unidentified low-energy scattered electron in the CAL [39].

5 Reconstruction of charm hadrons

The production yields of D^0, D^{*+}, D^+, D_s^+ and Λ_c^+ charm hadrons were measured in the range of transverse momentum $p_T(D, D^*, \Lambda_c) > 3.8\,\mathrm{GeV}$ and the range of pseudorapidity $|\eta(D, D^*, \Lambda_c)| < 1.6$. The p_T cut was imposed by trigger requirements and the η cut ensured a good acceptance in the CTD-MVD detector system. Charm hadrons were reconstructed using CTD-MVD tracks. Combinations of good tracks were used to form charm-hadron candidates, as detailed in the following sections. To ensure good momentum resolution, each track was required to reach at least the third superlayer of the CTD. The combinatorial background was significantly reduced by requiring $p_T(D, D^*)/E_T^{\theta>10^\circ} > 0.2$ and $p_T(\Lambda_c)/E_T^{\theta>10^\circ} > 0.25$ for charm mesons and baryons, respectively. The transverse energy was calculated as $E_T^{\theta>10^\circ} = \Sigma_{i,\theta_i>10^\circ}(E_i \sin\theta_i)$, where the sum runs over all energy deposits in the CAL with polar angles θ_i above 10°. A further background reduction was achieved by applying cuts on the minimal transverse momenta of the charm-hadron decay products. The large combinatorial background for the D^0, D^+ and D_s^+ mesons was additionally suppressed by secondary-decay vertex cuts (see section 5.1).

5.1 Reconstruction of D^0 mesons

The D^0 mesons were reconstructed using the decay mode $D^0 \to K^-\pi^+$. In each event, tracks with opposite charges and $p_T > 0.8\,\mathrm{GeV}$ were combined in pairs to form D^0 candidates. The nominal kaon and pion masses were assumed in turn for each track and the invariant mass of the pair, $M(K\pi)$, was calculated.

The kaon and pion tracks, measured precisely in the CTD-MVD detector system, were used to reconstruct the decay point of the D^0 meson. The relatively long lifetime of the D^0 meson resulted in a secondary vertex that is often well separated from the primary interaction point. This property was exploited to improve the signal-to-background ratio. The decay-length significance, S_l, was used as a discriminating variable. It is defined as $S_l = l/\sigma_l$, where l is the decay length in the transverse plane and σ_l is the uncertainty

JHEP09(2013)058

associated with this distance. The decay length is the distance in the transverse plane between the point of creation and decay vertex of the meson and is given by

$$l = \frac{\left(\vec{S}_{XY} - \vec{B}_{XY}\right) \cdot \vec{p}_T^{\,D}}{p_T^D}, \tag{5.1}$$

where $\vec{p}_T^{\,D}$ is the transverse momentum vector and $\vec{S}_{XY}$ is the two-dimensional position vector of the reconstructed decay vertex projected onto the XY plane. The vector $\vec{B}_{XY}$ points to the fitted geometrical centre of the beam-spot which is taken as the origin of the D meson. The centre of the elliptical beam-spot was determined using the average primary-vertex position for groups of a few thousand events. The vector $\vec{B}_{XY}$ was corrected for each event for the small difference in angle between the beam direction and the Z direction, using the Z position of the primary vertex of the event. The widths of the beam spot were 88 μm (80 μm) and 24 μm (22 μm) in the X and Y directions, respectively, for the e^+p (e^-p) data. The decay-length error, σ_l, was determined by folding the width of the beam-spot with the covariance matrix of the decay vertex after both were projected onto the D-meson momentum vector.

A cut $S_l > 1$ was applied. In addition, the χ^2 of the vertex fit was required to be less than 15; this quality cut was applied for all secondary D-meson decay-vertex fits in this paper.

For the selected D^0 candidates, a search was performed for a track that could be a "soft" pion, π_s, from a $D^{*+} \to D^0\pi_s^+$ decay. The soft pion was required to have $p_T > 0.2\,\text{GeV}$ and a charge opposite to that of the particle taken as a kaon. The corresponding D^0 candidate was assigned to the class of candidates "with ΔM tag" if the mass difference, $\Delta M = M(K\pi\pi_s) - M(K\pi)$, was in the range $0.143 < \Delta M < 0.148\,\text{GeV}$. All remaining D^0 candidates were assigned to the class of candidates "without ΔM tag".

For D^0 candidates with ΔM tag, the kaon and pion mass assignment was fixed according to the charge of the tracks. For D^0 candidates without ΔM tag, two mass assignments were assumed for each $K\pi$ pair, yielding two entries into the mass distribution: the true value, corresponding to the signal, and a wrong value, distributed over a broad range. To remove this background, the mass distribution, obtained for D^0 candidates with ΔM tag and assigning the wrong masses to the kaon and pion tracks, was subtracted from the $M(K\pi)$ distribution for all D^0 candidates without ΔM tag. The subtracted mass distribution was normalised to the ratio of numbers of D^0 mesons without and with ΔM tag obtained from the fit described below. Reflections from $D^0 \to K^-K^+$ and $D^0 \to \pi^-\pi^+$ decays were seen as two small bumps below and above the signal peak, respectively, of the $D^0 \to K^-\pi^+$ decay. They were subtracted using the simulated reflection shapes and normalised to the $D^0 \to K^-\pi^+$ signal according to the normalisation ratios observed in the simulation and using the PDG values of the respective branching ratios [43].

Figure 1 shows the $M(K\pi)$ distribution for D^0 candidates with and without ΔM tag obtained after the subtractions described above. Clear signals are seen at the nominal value of the D^0 mass in both distributions. The distributions were fitted simultaneously, assuming the same shape for the signals in both distributions. To describe the shape, a

JHEP09(2013)058

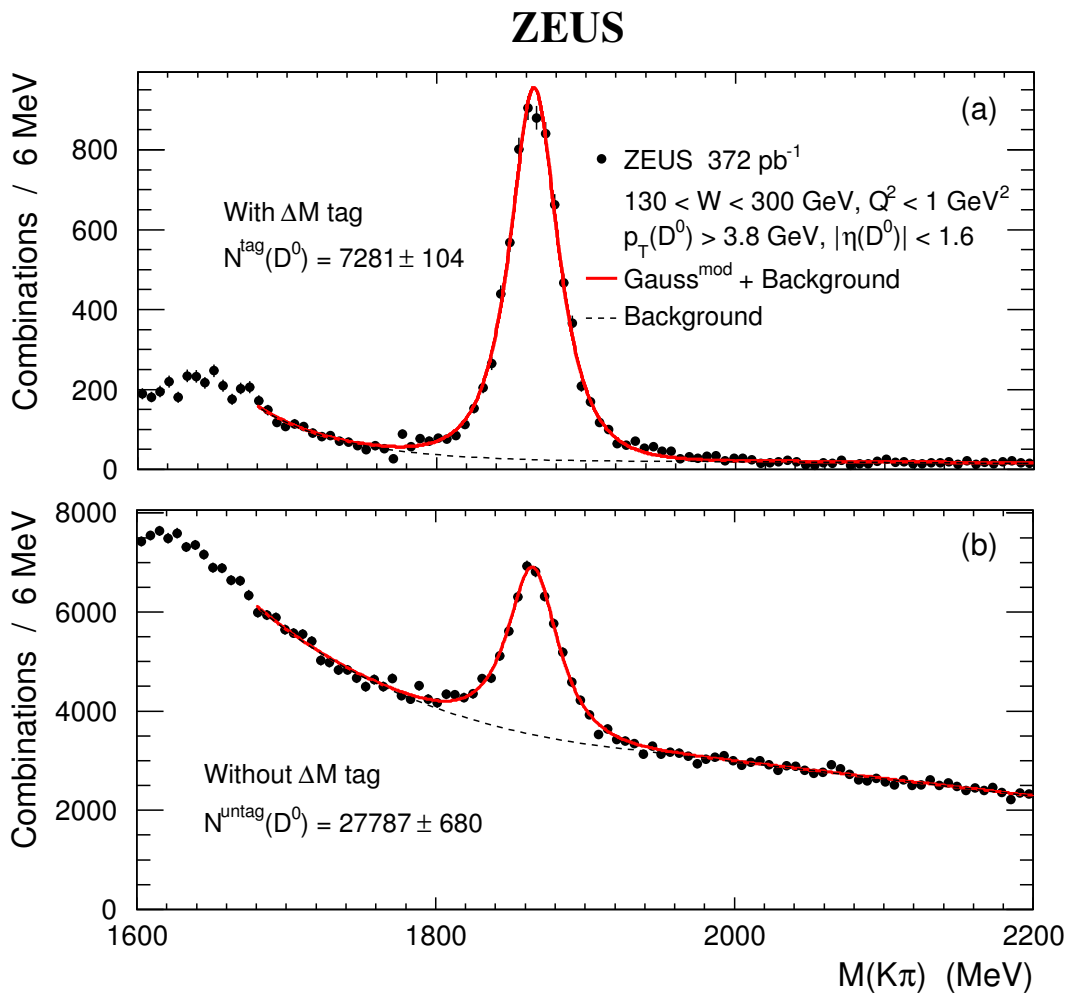

Figure 1. The $M(K\pi)$ distribution (dots) for (a) the D^0 candidates with ΔM tag, and for (b) the D^0 candidates without ΔM tag, obtained after the subtractions described in the text. The solid curves represent a fit to the sum of a modified Gaussian function and a background function (see text). The background is also shown separately (dashed curves).

modified Gaussian function was used:

$$\text{Gauss}^{\text{mod}} \propto \exp[-0.5 \cdot x^{1+1/(1+0.5\cdot x)}], \tag{5.2}$$

where $x = |[M(K\pi) - M_0]/\sigma|$. This functional form described both data and MC signals well. The signal position, M_0, and width, σ, and the number of D^0 mesons in each signal were free parameters of the fit. The background shape in both distributions is compatible with being approximately linear in the mass range above 1.92 GeV. For smaller $M(K\pi)$ values, there is an enhancement due to contributions from other D^0 decay modes and other D mesons, as was verified by the Monte Carlo simulation.

The background shape in the fit was described by the form $[A + B \cdot M(K\pi)]$ for $M(K\pi) > 1.92\,\text{GeV}$ and $[A+B\cdot M(K\pi)]\cdot\exp\{D\cdot[M(K\pi) - 1.92]^2\}$ for $M(K\pi) < 1.92\,\text{GeV}$.

JHEP09(2013)058

The free parameters A, B and D were assumed to be independent for the two $M(K\pi)$ distributions. The numbers of D^0 mesons yielded by the fit were $N^{\rm tag}(D^0) = 7281 \pm 104$ and $N^{\rm untag}(D^0) = 27787 \pm 680$ for selections with and without ΔM tag, respectively. The mass value obtained from the fit[3] was $1865.4 \pm 0.3\,\text{MeV}$ for the D^0 tagged and $1865.1 \pm 0.4\,\text{MeV}$ for the D^0 untagged samples, compared to the PDG value of $1864.83 \pm 0.14\,\text{MeV}$ [43].

5.2 Reconstruction of additional D^{*+} mesons

The $D^{*+} \to D^0\pi_s^+$ decays with $p_T(D^{*+}) > 3.8\,\text{GeV}$ and $|\eta(D^{*+})| < 1.6$ can be considered as a sum of two subsamples: decays with the D^0 having $p_T(D^0) > 3.8\,\text{GeV}$ and $|\eta(D^0)| < 1.6$, and decays with the D^0 outside that kinematic range. The former sample is represented by D^0 mesons reconstructed with ΔM tag, as discussed in the previous section. The latter sample of additional D^{*+} mesons was obtained using the same $D^0 \to K^-\pi^+$ decay channel and the selection described below.

In each event, tracks with opposite charges and $p_T > 0.4\,\text{GeV}$ were combined in pairs to form D^0 candidates. To calculate the invariant mass, $M(K\pi)$, kaon and pion masses were assumed in turn for each track. Only D^0 candidates which satisfy $1.81 < M(K\pi) < 1.92\,\text{GeV}$ were kept. Moreover, the D^0 candidates were required to have $p_T(D^0) < 3.8\,\text{GeV}$ or $|\eta(D^0)| > 1.6$. Any additional track with $p_T > 0.2\,\text{GeV}$ and a charge opposite to that of the kaon track was assigned the pion mass and combined with the D^0 candidate to form a D^{*+} candidate with invariant mass $M(K\pi\pi_s)$. The D^{*+} candidate was required to satisfy the cuts $p_T(D^{*+}) > 3.8\,\text{GeV}$ and $|\eta(D^{*+})| < 1.6$.

Figure 2 shows the $\Delta M = M(K\pi\pi_s) - M(K\pi)$ distribution for the D^{*+} candidates from the additional D^*-meson subsample after all cuts. A clear signal is seen at the nominal value of $M(D^{*+}) - M(D^0)$. The sum of the modified Gaussian function (eq. (5.2)) describing the signal and a function of the form $A \cdot (\Delta M - m_\pi)^B \cdot e^{-C\cdot\Delta M}$, describing the non-resonant background, was used to fit the data. Here m_π is the pion mass and A, B and C are free parameters of the fit. The fitted mass value[3] for the ΔM signal is $145.51 \pm 0.01\,\text{MeV}$, compared to the PDG value of $145.42 \pm 0.01\,\text{MeV}$ [43]. The number of reconstructed additional D^{*+} mesons determined from the fit was $N^{\rm add}(D^{*+}) = 2139 \pm 59$.

The combinatorial background was estimated also from the mass-difference distribution for wrong-charge combinations, in which both tracks forming the D^0 candidate had the same charge and the third track had the opposite charge. The number of reconstructed additional D^{*+} mesons was determined by subtracting the wrong-charge ΔM distribution after normalising it to the distribution of D^{*+} candidates with the appropriate charges in the range $0.151 < \Delta M < 0.167\,\text{GeV}$. The subtraction was performed in the signal range $0.143 < \Delta M < 0.148\,\text{GeV}$. The results obtained using the subtraction procedure instead of the fit were used to estimate the systematic uncertainty of the signal extraction.

5.3 Reconstruction of D^+ mesons

The D^+ mesons were reconstructed using the decay mode $D^+ \to K^-\pi^+\pi^+$. In each event, two tracks with the same charge and $p_T > 0.5\,\text{GeV}$ and a third track with the opposite

[3]For all fitted mass values in this paper the quoted uncertainties are only statistical.

JHEP09(2013)058

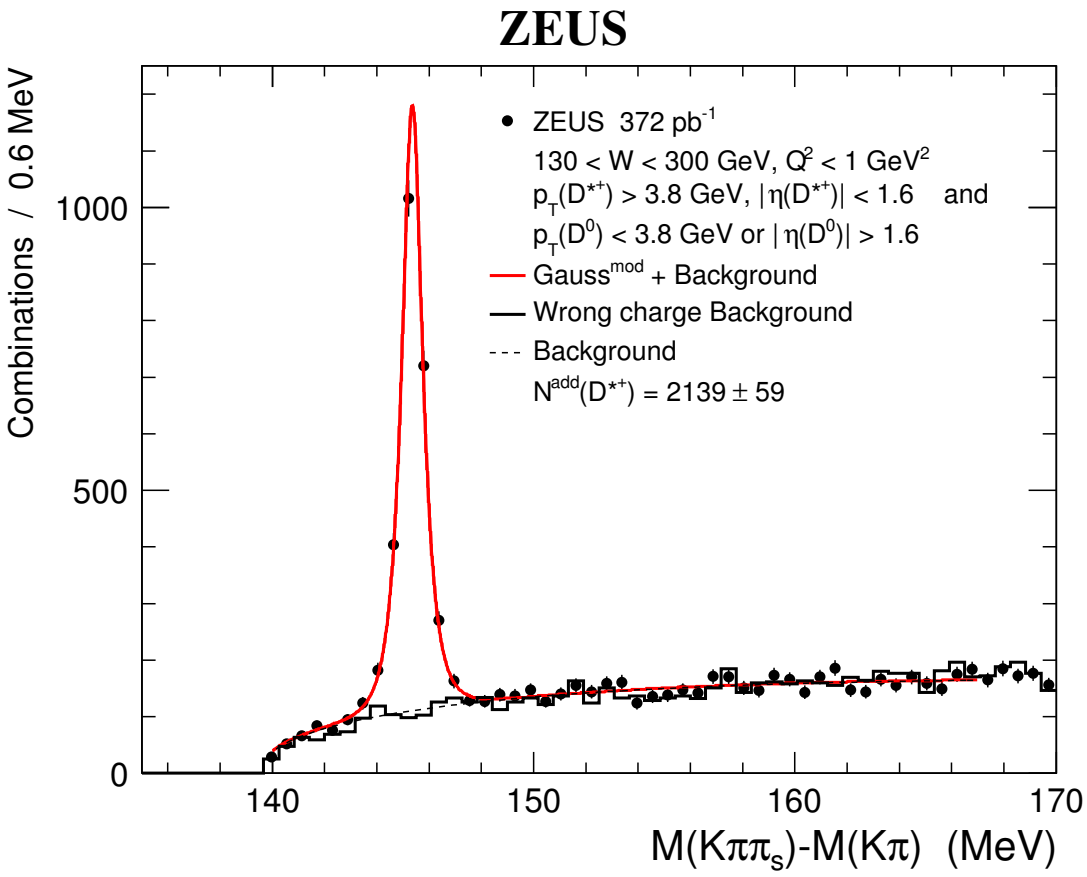

Figure 2. The distribution of the mass difference, $\Delta M = M(K\pi\pi_s) - M(K\pi)$, for the additional D^{*+} candidates (dots). The histogram solid shows the ΔM distribution for wrong-charge combinations. The solid curve represents a fit to the sum of a modified Gaussian function and a background function (see text). The background is also shown separately (dashed curve).

charge and $p_T > 0.7\,\text{GeV}$ were combined to form D^+ candidates. The pion mass was assigned to the two tracks with the same charge, the kaon mass was assigned to the third track, and the candidate invariant mass, $M(K\pi\pi)$, was calculated. To suppress background from D^{*+} decays, combinations with $M(K\pi\pi) - M(K\pi) < 0.15\,\text{GeV}$ were removed. The background from $D_s^+ \to \phi\pi^+$ with $\phi \to K^+K^-$ was suppressed by requiring that the invariant mass of any two tracks with opposite charges from D^+ candidates was not within ± 8 MeV of the ϕ mass [43] when the kaon mass was assigned to both tracks. To suppress combinatorial background, a cut on the decay-length significance for D^+ candidates was applied of $S_l > 3$.

Figure 3 shows the $M(K\pi\pi)$ distribution for the D^+ candidates after all cuts. A clear signal is seen at the nominal value of the D^+ mass. The sum of two Gaussian functions with the same peak position was used to describe the signal:

$$\text{Gauss}^{\text{sum}} = \frac{p_0}{\sqrt{2\pi}}\left[p_3/p_2 \cdot \exp[-(x-p_1)^2/2p_2^2] + (1-p_3)/p_4 \cdot \exp[-(x-p_1)^2/2p_4^2]\right], \quad (5.3)$$

where $x = M(K\pi\pi)$.

JHEP09(2013)058

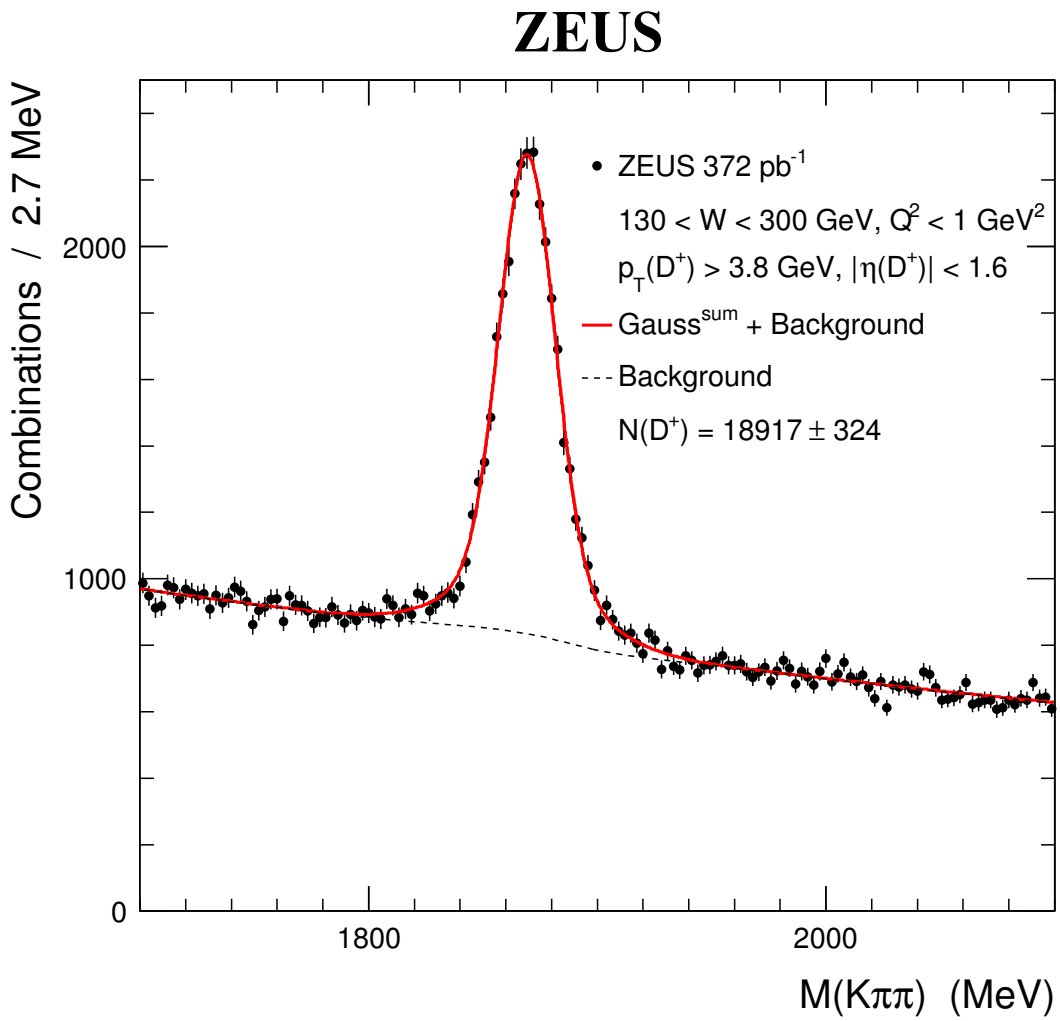

Figure 3. The $M(K\pi\pi)$ distribution for the D^+ candidates (dots). The solid curve represents a fit to the sum of two Gaussian functions and a background function. The background (dashed curve) is a sum of an exponential function and reflections from decays of other charm hadrons (see text). The reflections give rise to a small increase of the background in the signal region.

An exponential function describing the non-resonant background was used. Reflections caused by wrong mass assignments for the decay products of D_s^+ and Λ_c^+ decaying to three charged particles were added to the fit function using the simulated reflection shapes normalised to the measured D_s^+ and Λ_c^+ production rates. They give rise to a small increase of the background in the signal region. The number of reconstructed D^+ mesons yielded by the fit was $N(D^+) = 18917 \pm 324$. The fitted mass[3] of the D^+ was $1869.0 \pm 0.2\,\text{MeV}$, compared to the PDG value of $1869.62 \pm 0.15\,\text{MeV}$ [43].

5.4 Reconstruction of D_s^+ mesons

The D_s^+ mesons were reconstructed using the decay mode $D_s^+ \to \phi\pi^+$ with $\phi \to K^+K^-$. In each event, tracks with opposite charges and $p_T > 0.7\,\text{GeV}$ were assigned the kaon mass

JHEP09(2013)058

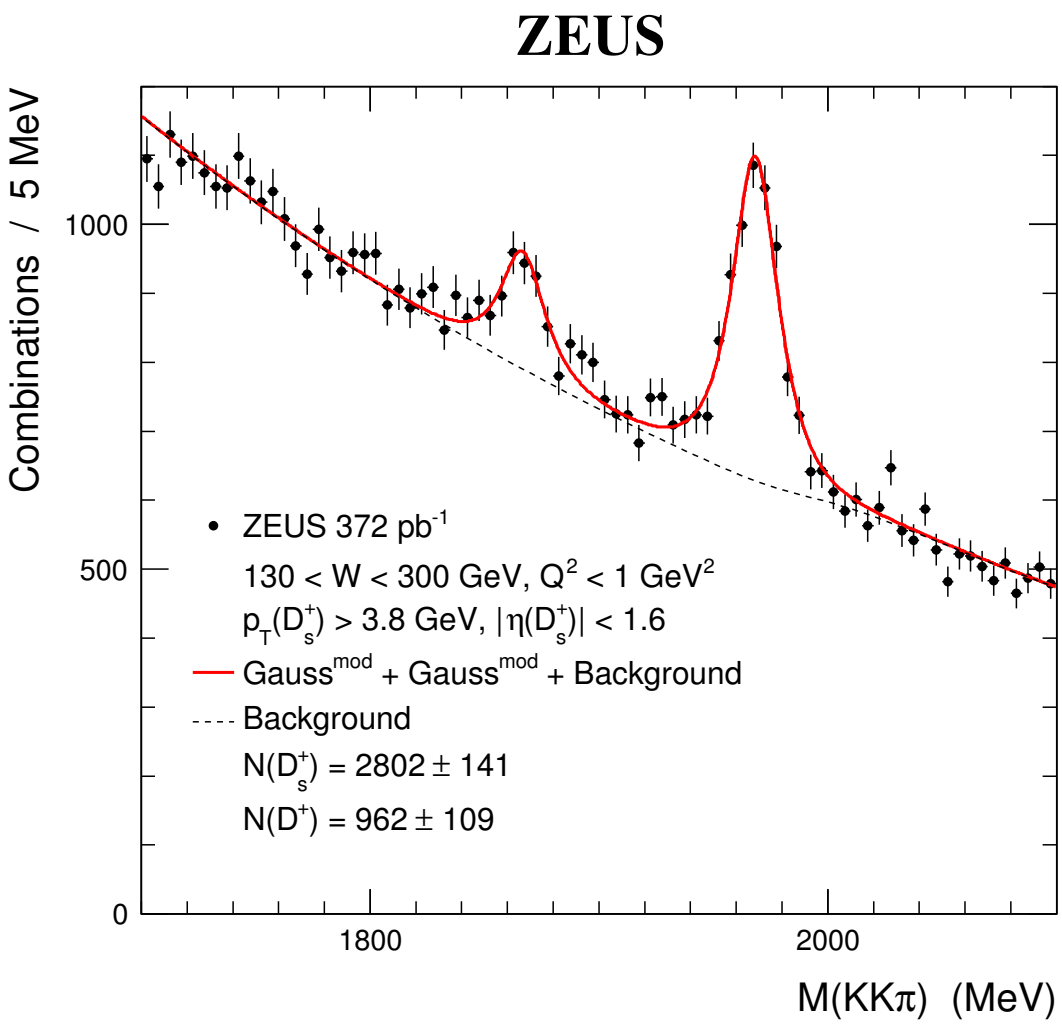

Figure 4. The $M(KK\pi)$ distribution for the D_s^+ candidates (dots). The solid curve represents a fit to the sum of two modified Gaussian functions and a background function. The peak at 1870 MeV is due to the decay $D^+ \to K^+K^-\pi^+$. The background (dashed curve) is a sum of an exponential function and reflections from decays of other charm hadrons (see text).

and combined in pairs to form ϕ candidates. The ϕ candidate was kept if its invariant mass, $M(KK)$, was within ± 8 MeV of the ϕ mass [43]. Any additional track with $p_T > 0.5\,\text{GeV}$ was assigned the pion mass and combined with the ϕ candidate to form a D_s^+ candidate with invariant mass $M(KK\pi)$. The cut on the decay-length significance for D_s^+ candidates was $S_l > 0$.

Figure 4 shows the $M(KK\pi)$ distribution for the D_s^+ candidates after all cuts. A clear signal is seen at the nominal D_s^+ mass. There is also a smaller signal around the nominal D^+ mass as expected from the decay $D^+ \to \phi\pi^+$ with $\phi \to K^+K^-$. The mass distribution was fitted by the sum of two modified Gaussian functions (eq. (5.2)) describing the signals and an exponential function describing the non-resonant background. To reduce the number of free fit parameters in the fit, the ratio of the widths of the D^+ and D_s^+ signals

JHEP09(2013)058

was fixed to the value observed in the MC simulation. Reflections arising from wrong mass assignments for the decay products of D^+ and Λ_c^+ decays to three charged particles were added to the fit function using the simulated reflection shapes normalised to the measured D^+ and Λ_c^+ production rates. The number of reconstructed D_s^+ mesons yielded by the fit was $N(D_s^+) = 2802 \pm 141$. The fitted mass[3] of the D_s^+ was $1968.0 \pm 0.5\,\text{MeV}$, compared to the PDG value of $1968.49 \pm 0.32\,\text{MeV}$ [43].

5.5 Reconstruction of Λ_c^+ baryons

The Λ_c^+ baryons were reconstructed using the decay mode $\Lambda_c^+ \to K^- p \pi^+$. In each event, two same-charge tracks and a third track with opposite charge were combined to form Λ_c^+ candidates. Due to the large difference between the proton and pion masses and the high Λ_c^+ momentum, the proton momentum is typically larger than that of the pion. Therefore, the proton (pion) mass was assigned to the track of the same-charge pair with the larger (smaller) momentum. The kaon mass was assigned to the third track and the invariant mass, $M(Kp\pi)$, was calculated. Only candidates with $p_T(K) > 0.5\,\text{GeV}$, $p_T(p) > 1.3\,\text{GeV}$ and $p_T(\pi) > 0.5\,\text{GeV}$ were kept. Reflections from D^+ and D_s^+ decays to three charged particles were subtracted from the $M(Kp\pi)$ spectrum using the simulated reflection shapes normalised to the measured D^+ and D_s^+ production rates.

Figure 5 shows the $M(Kp\pi)$ distribution for the Λ_c^+ candidates after all cuts, obtained after the reflection subtraction. A clear signal is seen at the nominal Λ_c^+ mass. The sum of a modified Gaussian function (eq. (5.2)) describing the signal and a background function parametrised as

$$\exp[A \cdot M(Kp\pi) + B] \cdot M(Kp\pi)^C,$$

where A, B and C are free parameters, was fitted to the mass distribution. The width parameter of the modified Gaussian was fixed to $\sigma = 10$ MeV. This value corresponds to the width determined in the MC, multiplied by a factor 1.11. The uncertainty of this number is taken into account in the systematics variations. The factor 1.11 corrects for the difference of the observed width of the $D^+ \to K^-\pi^+\pi^+$ signal between data and simulation. The number of reconstructed Λ_c^+ baryons yielded by the fit was $N(\Lambda_c^+) = 7682 \pm 964$. The fitted mass[3] of the Λ_c^+ was $2290 \pm 1.8\,\text{MeV}$, compared to the PDG value of $2286.46 \pm 0.14\,\text{MeV}$ [43].

6 Charm-hadron production cross sections

The cross sections for the production of the various charm hadrons were determined, but the fragmentation fractions involve only ratios, in which common normalisation uncertainties cancel.

The fraction of charm quarks hadronising as a particular charm hadron, $f(c \to D, D^*, \Lambda_c)$, is given by the ratio of the production cross section for the hadron to the sum of the production cross sections for all charm ground states. The charm-hadron cross sections were determined for the process $ep \to e(D, D^*, \Lambda_c)X$ in the kinematic region $Q^2 < 1\,\text{GeV}^2$, $130 < W < 300\,\text{GeV}$, $p_T(D, D^*, \Lambda_c) > 3.8\,\text{GeV}$ and $|\eta(D, D^*, \Lambda_c)| < 1.6$.

JHEP09(2013)058

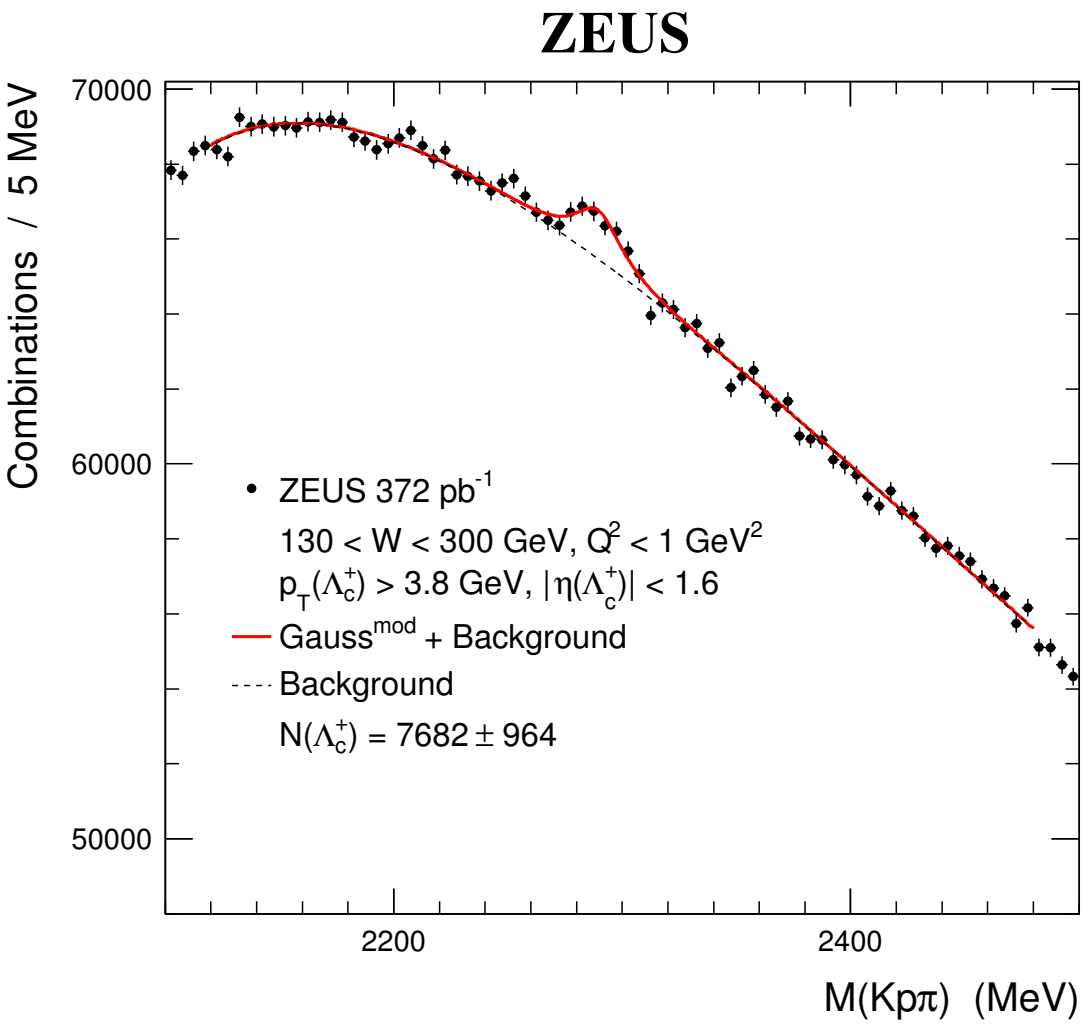

Figure 5. The $M(Kp\pi)$ distribution for the Λ_c candidates (dots), obtained after reflection subtraction (see text). The solid curve represents a fit to the sum of a modified Gaussian function and a background function (see text). The background is also shown separately (dashed curve).

The cross section for a given charm hadron was calculated from

$$\sigma(D, D^*, \Lambda_c) = \frac{N^{\rm data}_{(D,D^*,\Lambda_c)} - s_b \cdot N^{b,\rm MC}_{(D,D^*,\Lambda_c)}}{\mathcal{A} \cdot \mathcal{L} \cdot \mathcal{B}}\,, \tag{6.1}$$

where $N^{\rm data}_{(D,D^*,\Lambda_c)}$ denotes the number of reconstructed charm hadrons in the data, $\mathcal{A}$ the acceptance for this charm hadron, $\mathcal{L}$ the integrated luminosity and $\mathcal{B}$ the branching ratio or the product of the branching ratios [43] for the decay channels used in the reconstruction. The Pythia MC sample of charm photoproduction (see section 3) was used to evaluate the acceptance. The contributions from beauty-hadron decays were subtracted using the prediction from Pythia. For this purpose, the branching ratios of beauty-quark decays to the charmed hadrons were corrected in the MC, using the correction factors [1] based on the values measured at LEP [44, 45]. Finally, the number of reconstructed charm hadrons

JHEP09(2013)058

from beauty, $N^{b,\mathrm{MC}}_{D,D^*,\Lambda_c}$, in the MC, normalised to the data luminosity and multiplied by a scale factor, s_b, was subtracted from the data (eq. (6.1)). The scale factor was chosen as $s_b = 1.5 \pm 0.5$, an average value which was estimated from ZEUS measurements [46–48] of beauty photoproduction.

Using the number of reconstructed signal events (see section 5), the following cross sections for the sum of each charm hadron and its antiparticle were calculated:

- for D^0 mesons not originating from $D^{*+} \to D^0\pi_s^+$ decays, $\sigma^{\mathrm{untag}}(D^0)$;
- for D^0 mesons from $D^{*+} \to D^0\pi_s^+$ decays, $\sigma^{\mathrm{tag}}(D^0)$. The ratio $\sigma^{\mathrm{tag}}(D^0)/\mathcal{B}_{D^{*+}\to D^0\pi^+}$ gives the D^{*+} cross section, $\sigma(D^{*+})$, corresponding to D^0 production in the kinematic range $p_T(D^0) > 3.8\,\mathrm{GeV}$ and $|\eta(D^0)| < 1.6$ for the $D^{*+} \to D^0\pi_s^+$ decay. Here $\mathcal{B}_{D^{*+}\to D^0\pi^+} = 0.677$ is the branching ratio of the $D^{*+} \to D^0\pi_s^+$ decay [43];
- for additional D^{*+} mesons, $\sigma^{\mathrm{add}}(D^{*+})$. The sum $\sigma^{\mathrm{tag}}(D^0)/\mathcal{B}_{D^{*+}\to D^0\pi^+} + \sigma^{\mathrm{add}}(D^{*+})$ gives the D^{*+} cross section, $\sigma^{\mathrm{kin}}(D^{*+})$, corresponding to D^{*+} production in the kinematic range $p_T(D^{*+}) > 3.8\,\mathrm{GeV}$ and $|\eta(D^{*+})| < 1.6$;
- for D^+ mesons, $\sigma(D^+)$;
- for D_s^+ mesons, $\sigma(D_s^+)$;
- for Λ_c^+ baryons, $\sigma(\Lambda_c^+)$.

7 Systematic uncertainties

The systematic uncertainties were determined by changing the analysis procedure or by varying parameter values within their estimated uncertainties. The following systematic uncertainty sources were considered:

- $\{\delta_1\}$ the uncertainty of the beauty subtraction (see section 6) was determined by varying the scale factor s_b for the Pythia MC prediction by ± 0.5 from the nominal value $s_b = 1.5$. This was done to account for the range of the Pythia beauty-prediction scale factors extracted in various analyses [46–48]. In addition the branching ratios of b quarks to charm hadrons were varied by their uncertainties [44, 45];
- $\{\delta_2\}$ the uncertainty in the rate of the charm-strange baryons (see section 8.2) was determined by varying the normalisation factor for the Λ_c^+ production cross section by its estimated uncertainty [1] of ± 0.05 from the nominal value 1.14;
- $\{\delta_3\}$ the uncertainties related to the signal extraction procedures (see sections 5.1–5.5) were obtained by the following (independent) variations:
  - for the D^0 signals with and without ΔM tag: the background parametrisation was changed: for the region $M(K\pi) < 1.92$ GeV a linear term $C\cdot[M(K\pi) - 1.92]$ was added to the argument of the exponential function; the transition point for the parametrisation was moved from 1.92 GeV to 1.84 GeV. The fit range was narrowed by 50 MeV on both sides;

JHEP09(2013)058

– for the additional D^{*+} signal: the $M(K\pi)$ mass window for the selected D^0 candidates was narrowed by 5.5 MeV on both sides. The range used for the fit of the ΔM distribution was narrowed by 1 MeV (left) and 5 MeV (right);

The wrong-charge subtraction procedure was used instead of the fit; the range used for the normalisation of the wrong-charge background was narrowed by 1 MeV (left) and 5 MeV (right); the signal range used for the wrong-charge subtraction was narrowed or broadened by 1 MeV on both sides;

– for the D^+ signal: a modified Gaussian was used as an alternative parametrisation for the signal; the background parametrisation was changed to a parabola. The fit range was narrowed by 50 MeV on both sides;

– for the D_s^+ signal: the background parametrisation was changed to a parabola. The fit range was narrowed by 50 MeV (left) and 30 MeV (right);

– for the Λ_c^+ signal: the background parametrisation was changed to a cubic polynomial. The fit range was narrowed by 30 MeV on both sides. The width parameter σ of the modified Gaussian (eq. (5.2)) was varied by ±10% from its nominal value, a conservative estimate of its uncertainty. Further cross checks were performed: the width of the modified Gaussian was used as a free fit parameter; the mass of the Λ_c^+ was fixed to the PDG value [43]. The resulting signal-yield changes from these two variations were negligible.

The uncertainties arising from the various reflections in the mass spectra (see section 5) were evaluated by varying the size of each reflection conservatively by ±20%.

The largest contribution to the signal extraction procedures was the change of the background parametrisation;

- $\{\delta_4\}$ the model dependence of the acceptance corrections was estimated by varying the reweighting of the MC kinematic distributions (see section 3) until clear discrepancies became visible between the shapes observed in the data and in the MC;

- $\{\delta_5\}$ the uncertainty of the trigger efficiency was evaluated by comparing the fitted signal yields taken with independent triggers. This uncertainty largely cancels in the fragmentation fractions;

- $\{\delta_6\}$ the overestimate of the track-finding efficiency in the MC relative to that in the data was estimated to be at most 2%. This leads to a possible underestimation of the production cross sections for the charm hadrons with two (three) decay tracks by a factor 1.02^2 (1.02^3) which was taken into account for the systematics of the fragmentation fractions;

- $\{\delta_7\}$ the uncertainty of the CAL simulation was determined by varying the simulation: the CAL energy scale was changed by ±2% and the CAL energy resolution by ±20% of its value;

- $\{\delta_8\}$ the uncertainty related to the S_l cut was determined by changing the value of the cut to $S_l > 4$ for D^+ and by omitting the S_l cut for D^0 and D_s^+.

JHEP09(2013)058

	total (%)	δ_1 (%)	δ_2 (%)	δ_3 (%)	δ_4 (%)	δ_5 (%)	δ_6 (%)	δ_7 (%)	δ_8 (%)
$f(c \to D^+)$	$^{+1.8}_{-2.7}$	$^{+0.3}_{-0.3}$	$^{+0.4}_{-0.4}$	$^{+1.4}_{-2.0}$	$^{+0.3}_{-0.3}$	$^{+0.6}_{-0.6}$	$+1.0$	$^{+0.2}_{-1.6}$	$^{+0.2}_{-0.1}$
$f(c \to D^0)$	$^{+1.7}_{-1.0}$	$^{+0.2}_{-0.2}$	$^{+0.4}_{-0.4}$	$^{+1.6}_{-0.6}$	$^{+0.1}_{-0.1}$	$^{+0.3}_{-0.3}$	-0.7	$+0.8$	$^{+0.2}_{-0.1}$
$f(c \to D_s^+)$	$^{+2.1}_{-8.0}$	$^{+0.4}_{-0.4}$	$^{+0.4}_{-0.3}$	$^{+1.3}_{-7.6}$	$^{+0.1}_{-0.1}$	$^{+0.8}_{-0.9}$	$+1.1$	$^{+0.3}_{-1.9}$	$^{+0.2}_{-0.1}$
$f(c \to \Lambda_c^+)$	$^{+6.4}_{-11.7}$	$^{+0.1}_{-0.1}$	$^{+0.4}_{-0.3}$	$^{+6.1}_{-11.6}$	$^{+0.2}_{-0.1}$	$^{+1.1}_{-0.4}$	$+1.0$	$^{+0.5}_{-0.9}$	-0.7
$f(c \to D^{*+})$	$^{+1.9}_{-1.9}$	$^{+1.0}_{-1.0}$	$^{+0.4}_{-0.4}$	$^{+1.5}_{-1.6}$	$^{+0.2}_{-0.1}$	$^{+0.4}_{-0.4}$	-0.4	$^{+0.3}_{-0.1}$	$+0.2$

Table 1. The total and individual δ_1–δ_8 (see text) systematic uncertainties for the charm-hadron fragmentation fractions.

Contributions from the different systematic uncertainties were calculated and added in quadrature separately for positive and negative variations. The total and individual systematic uncertainties δ_1 to δ_8 for the charm fragmentation fractions are summarised in table 1.

The largest systematic uncertainties are related to the signal-extraction procedures.

8 Results

8.1 Equivalent phase-space treatment

To compare the inclusive D^+ and D^0 cross sections with each other and with the inclusive D^{*+} cross section, it is necessary to take into account that in the D^* decay only a fraction of the parent D^* momentum is transferred to the daughter D meson. For such a comparison, the "equivalent" D^+ and D^0 cross sections, $\sigma^{\rm eq}(D^+)$ and $\sigma^{\rm eq}(D^0)$, were defined [1] as the cross section for D^+ and D^0 production including the contributions from D^* decay, plus the contribution from additional D^* mesons (see section 5.2). The cross section for D^+ and D^0 production is $\sigma(D^+)$ and $\sigma^{\rm tag}(D^0) + \sigma^{\rm untag}(D^0)$, respectively. The contributions from additional D^* mesons are, for the D^+ meson,

$$\sigma^{\rm add}(D^+) = \sigma^{\rm add}(D^{*+}) \cdot (1 - B_{D^{*+}\to D^0\pi^+})$$

and for the D^0 meson

$$\sigma^{\rm add}(D^0) = \sigma^{\rm add}(D^{*+}) B_{D^{*+}\to D^0\pi^+} + \sigma^{\rm add}(D^{*0}),$$

noting that D^{*0} decays always to D^0 [43].

The cross-section $\sigma^{\rm add}(D^{*0})$ is not measured and is determined as

$$\sigma^{\rm add}(D^{*0}) = \sigma^{\rm add}(D^{*+}) \cdot R_{u/d}, \tag{8.1}$$

where $R_{u/d}$ is the ratio of neutral to charged D-meson production rates. It is given by the ratio of the sum of D^{*0} and direct D^0 production to the sum of D^{*+} and direct D^+ production cross sections. It can be written as [1]

$$R_{u/d} = \frac{\sigma^{\rm untag}(D^0)}{\sigma(D^+) + \sigma^{\rm tag}(D^0)}. \tag{8.2}$$

JHEP09(2013)058

Combining everything produces the following expressions for $\sigma^{\rm eq}(D^+)$ and $\sigma^{\rm eq}(D^0)$:

$$\sigma^{\rm eq}(D^+) = \sigma(D^+) + \sigma^{\rm add}(D^+) = \sigma(D^+) + \sigma^{\rm add}(D^{*+}) \cdot (1 - B_{D^{*+}\to D^0\pi^+})$$

and

$$\begin{aligned}\sigma^{\rm eq}(D^0) &= \sigma^{\rm untag}(D^0) + \sigma^{\rm tag}(D^0) + \sigma^{\rm add}(D^0) \\ &= \sigma^{\rm untag}(D^0) + \sigma^{\rm tag}(D^0) + \sigma^{\rm add}(D^{*+})B_{D^{*+}\to D^0\pi^+} + \sigma^{\rm add}(D^{*0}),\end{aligned}$$

which together with eq. (8.1) gives

$$\sigma^{\rm eq}(D^0) = \sigma^{\rm untag}(D^0) + \sigma^{\rm tag}(D^0) + \sigma^{\rm add}(D^{*+}) \cdot (B_{D^{*+}\to D^0\pi^+} + R_{u/d}).$$

The observable $R_{u/d}$ was measured in the kinematic region $Q^2 < 1\,\text{GeV}^2$, $130 < W < 300\,\text{GeV}$, $p_T(D) > 3.8\,\text{GeV}$ and $|\eta(D)| < 1.6$. The value obtained from eq. (8.2) is

$$R_{u/d} = 1.09 \pm 0.03\,(\text{stat.})^{+0.04}_{-0.03}\,(\text{syst.}) \pm 0.02\,(\text{br}),$$

where the last uncertainty arises from the uncertainties of the branching ratios used. The result is in agreement with the previous measurement [1] and slightly above but still compatible with $R_{u/d} = 1$, expected from isospin invariance in the kinematic range of this measurement.

Monte Carlo studies performed for the previous ZEUS measurement [1] showed that this equivalent phase-space treatment for the non-strange D and D^* mesons minimises differences between the fragmentation fractions measured in the accepted $p_T(D, D^*, \Lambda_c)$ and $\eta(D, D^*, \Lambda_c)$ kinematic region and those in the full phase space. The extrapolation factors using the Pythia MC with either the Peterson or Bowler fragmentation function were generally close to unity to within a few percent [1].

8.2 Charm fragmentation fractions

For the determination of the fragmentation fractions of the D^0, D^+, D_s^+ and Λ_c^+ charm ground states, the total cross section for charmed hadron production is needed. In this cross section, the production cross sections of the charm-strange baryons Ξ_c^+, Ξ_c^0 and Ω_c^0 must also be included. Since these charm-strange baryons do not decay into Λ_c^+, a correction is needed. The production rates for these baryons are expected to be much lower than that of the Λ_c^+ due to strangeness suppression. The relative rates for the ground states of the charm-strange baryons were estimated from the non-charm sector following the LEP procedure [49]. The total rate for the three charm-strange baryons relative to the Λ_c^+ state is expected to be about 14% [1]. Therefore the Λ_c^+ production cross section was scaled by the factor 1.14.

Using the equivalent D^0 and D^+ cross sections, the sum of the production cross sections for all open-charm ground states, $\sigma_{\rm gs}$, is given by

$$\sigma_{\rm gs} = \sigma^{\rm eq}(D^+) + \sigma^{\rm eq}(D^0) + \sigma(D_s^+) + \sigma(\Lambda_c^+) \cdot 1.14,$$

JHEP09(2013)058

	ZEUS (γp) HERA II	ZEUS (γp) [1] HERA I	ZEUS (DIS) [3,4] HERA I
	stat. syst. br.	stat. syst. br.	stat. syst. br.
$f(c \to D^+)$	$0.234 \pm 0.006\ ^{+0.004}_{-0.006}\ ^{+0.006}_{-0.008}$	$0.222 \pm 0.015\ ^{+0.014}_{-0.005}\ ^{+0.011}_{-0.013}$	$0.217 \pm 0.018\ ^{+0.002}_{-0.019}\ ^{+0.009}_{-0.010}$
$f(c \to D^0)$	$0.588 \pm 0.017\ ^{+0.011}_{-0.006}\ ^{+0.012}_{-0.018}$	$0.532 \pm 0.022\ ^{+0.018}_{-0.017}\ ^{+0.019}_{-0.028}$	$0.585 \pm 0.019\ ^{+0.009}_{-0.052}\ ^{+0.018}_{-0.019}$
$f(c \to D_s^+)$	$0.088 \pm 0.006\ ^{+0.002}_{-0.007}\ ^{+0.005}_{-0.005}$	$0.075 \pm 0.007\ ^{+0.004}_{-0.004}\ ^{+0.005}_{-0.005}$	$0.086 \pm 0.010\ ^{+0.007}_{-0.008}\ ^{+0.005}_{-0.005}$
$f(c \to \Lambda_c^+)$	$0.079 \pm 0.013\ ^{+0.005}_{-0.009}\ ^{+0.024}_{-0.014}$	$0.150 \pm 0.023\ ^{+0.014}_{-0.022}\ ^{+0.038}_{-0.025}$	$0.098 \pm 0.027\ ^{+0.020}_{-0.017}\ ^{+0.025}_{-0.023}$
$f(c \to D^{*+})$	$0.234 \pm 0.006\ ^{+0.004}_{-0.004}\ ^{+0.005}_{-0.007}$	$0.203 \pm 0.009\ ^{+0.008}_{-0.006}\ ^{+0.007}_{-0.010}$	$0.234 \pm 0.011\ ^{+0.006}_{-0.021}\ ^{+0.007}_{-0.010}$

	H1 (DIS) [2]	Combined e^+e^- data [5–16]
	stat.$\oplus$syst. br.	stat.$\oplus$syst. br.
$f(c \to D^+)$	$0.204 \pm 0.026\ ^{+0.009}_{-0.010}$	$0.222\ \pm 0.010\ ^{+0.010}_{-0.009}$
$f(c \to D^0)$	$0.584 \pm 0.048\ ^{+0.018}_{-0.019}$	$0.544\ \pm 0.022\ ^{+0.007}_{-0.007}$
$f(c \to D_s^+)$	$0.121 \pm 0.044\ ^{+0.008}_{-0.008}$	$0.077\ \pm 0.006\ ^{+0.005}_{-0.004}$
$f(c \to \Lambda_c^+)$		$0.076\ \pm 0.007\ ^{+0.027}_{-0.016}$
$f(c \to D^{*+})$	$0.276 \pm 0.034\ ^{+0.009}_{-0.012}$	$0.235\ \pm 0.007\ ^{+0.003}_{-0.003}$

Table 2. Fractions of charm quarks hadronising as a particular charm hadron, $f(c \to D, D^*, \Lambda_c)$. The fractions are shown for the D^+, D^0, D_s^+ and Λ_c^+ charm ground states and for the D^{*+} state. The fractions in this and the previous ZEUS paper [1] were determined for the kinematic range $p_T > 3.8\,\text{GeV}$, $|\eta| < 1.6$ and $130 < W < 300\,\text{GeV}$. Data for previous results [1,16] were updated to 2010 branching ratios [17,50,51]; data from this paper were calculated with 2012 branching ratios [43].

which can be expressed using $R_{u/d}$ from eq. (8.2) as

$$\sigma_{\text{gs}} = \sigma(D^+) + \sigma^{\text{untag}}(D^0) + \sigma^{\text{tag}}(D^0) + \sigma^{\text{add}}(D^{*+}) \cdot (1 + R_{u/d}) + \sigma(D_s^+) + \sigma(\Lambda_c^+) \cdot 1.14.$$

The fragmentation fractions for the measured charm ground states and for D^{*+} are given by

$$\begin{aligned}
f(c \to D^+) &= \sigma^{\text{eq}}(D^+)/\sigma_{\text{gs}} = [\sigma(D^+) + \sigma^{\text{add}}(D^{*+}) \cdot (1 - \mathcal{B}_{D^{*+} \to D^0\pi^+})]/\sigma_{\text{gs}}, \\
f(c \to D^0) &= \sigma^{\text{eq}}(D^0)/\sigma_{\text{gs}} \\
&= [\sigma^{\text{untag}}(D^0) + \sigma^{\text{tag}}(D^0) + \sigma^{\text{add}}(D^{*+}) \cdot (R_{u/d} + \mathcal{B}_{D^{*+} \to D^0\pi^+})]/\sigma_{\text{gs}}, \\
f(c \to D_s^+) &= \sigma(D_s^+)/\sigma_{\text{gs}}, \\
f(c \to \Lambda_c^+) &= \sigma(\Lambda_c^+)/\sigma_{\text{gs}}, \\
f(c \to D^{*+}) &= \sigma^{\text{kin}}(D^{*+})/\sigma_{\text{gs}} = [\sigma^{\text{tag}}(D^0)/\mathcal{B}_{D^{*+} \to D^0\pi^+} + \sigma^{\text{add}}(D^{*+})]/\sigma_{\text{gs}}.
\end{aligned}$$

The charm fragmentation fractions, measured in the kinematic region $Q^2 < 1\,\text{GeV}^2$, $130 < W < 300\,\text{GeV}$, $p_T(D, D^*, \Lambda_c) > 3.8\,\text{GeV}$ and $|\eta(D, D^*, \Lambda_c)| < 1.6$, are summarised in table 2. These results have been computed using the PDG 2012 branching-ratio

JHEP09(2013)058

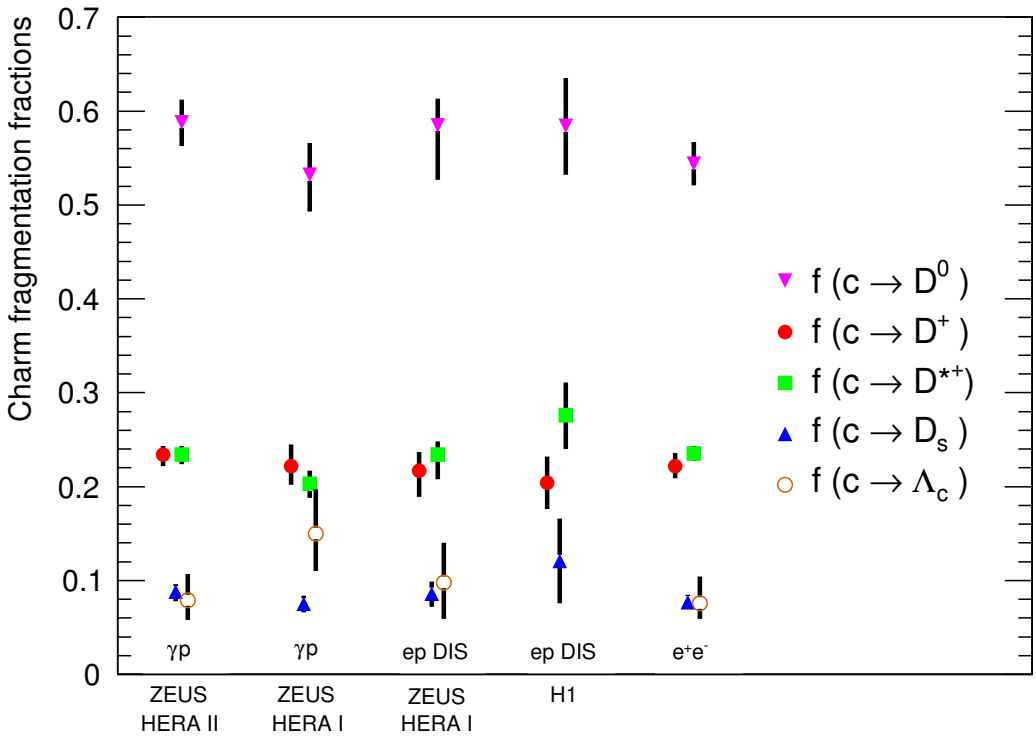

Figure 6. Fractions of charm quarks hadronising as a particular charm hadron. The photoproduction measurements presented in this paper are shown (first column) and compared to previous HERA results in photoproduction (second column), DIS (third and fourth column) and to e^+e^- data (last column), with statistical, systematic and branching-ratio uncertainties added in quadrature.

values [43]. The measurements are compared to previous HERA results [1–4] and to the combined fragmentation fractions for charm production in e^+e^- annihilations compiled previously [16] and updated [17, 50] with the 2010 branching-ratio values [51]. This comparison is also shown in figure 6. The obtained precision of the fragmentation fractions is competitive with measurements in e^+e^- collisions. All data from ep and e^+e^- collisions are in agreement with each other. This demonstrates that the fragmentation fractions of charm quarks are independent of the production process and supports the hypothesis of universality of heavy-quark fragmentation.

The charm fragmentation fractions can also be used [1] to determine the fraction of charged D mesons produced in a vector state, P_v^d, and the strangeness-suppression factor, γ_s:

$$P_v^d = \frac{\sigma^{\mathrm{kin}}(D^{*+})}{\sigma^{\mathrm{kin}}(D^{*+}) + \sigma^{\mathrm{dir}}(D^{+})} = \frac{\sigma^{\mathrm{tag}}(D^0)/\mathcal{B}_{D^{*+}\to D^0\pi^+} + \sigma^{\mathrm{add}}(D^{*+})}{\sigma(D^+) + \sigma^{\mathrm{tag}}(D^0) + \sigma^{\mathrm{add}}(D^{*+})}$$

and

$$\gamma_s = \frac{2\sigma(D_s^+)}{\sigma^{\mathrm{eq}}(D^+) + \sigma^{\mathrm{eq}}(D^0)}.$$

JHEP09(2013)058

The value of P_v^d obtained is

$$P_v^d = 0.595 \pm 0.020(\text{stat.}) \pm 0.015(\text{syst.}) \pm 0.011(\text{br.}).$$

This is consistent with the result from the previous publication [1] and with the result from combined e^+e^- data [16, 17]. It is smaller than the naive spin-counting prediction of 0.75 and also smaller than 2/3, the value predicted by the string-fragmentation approach [52].

The strangeness-suppression factor obtained is

$$\gamma_s = 0.214 \pm 0.013(\text{stat.})^{+0.006}_{-0.017}(\text{syst.}) \pm 0.012(\text{br.}),$$

consistent with the result from the previous publication [1]. It is interesting to compare this value with values derived from kaon and lambda production, which are between 0.22 and 0.3 [53–57].

9 Summary

The photoproduction of the charm hadrons D^0, D^{*+}, D^+, D_s^+ and Λ_c^+ and their corresponding antiparticles has been measured with the ZEUS detector in in the kinematic range $p_T(D, D^*, \Lambda_c) > 3.8\,\text{GeV}$, $|\eta(D, D^*, \Lambda_c)| < 1.6$, $130 < W < 300\,\text{GeV}$ and $Q^2 < 1\,\text{GeV}^2$.

Using a data set with an integrated luminosity of 372 pb^{-1}, the fractions of charm quarks hadronising as D^0, D^{*+}, D^+, D_s^+ and Λ_c^+ hadrons have been determined. In addition, the ratio of neutral to charged D-meson production rates, the fraction of charged D mesons produced in a vector state, and the strangeness-suppression factor have been determined.

The precision of the fragmentation fractions obtained is competitive with measurements in e^+e^- collisions. All data from ep and e^+e^- collisions are in agreement with each other. This demonstrates that the fragmentation fractions of charm quarks are independent of the production process and supports the hypothesis of the universality of heavy-quark fragmentation.

Acknowledgments

We appreciate the contributions to the construction and maintenance of the ZEUS detector of many people who are not listed as authors. The HERA machine group and the DESY computing staff are especially acknowledged for their success in providing excellent operation of the collider and the data-analysis environment. We thank the DESY directorate for their strong support and encouragement.

Open Access. This article is distributed under the terms of the Creative Commons Attribution License which permits any use, distribution and reproduction in any medium, provided the original author(s) and source are credited.

JHEP09(2013)058

References

[1] ZEUS collaboration, S. Chekanov et al., *Measurement of charm fragmentation ratios and fractions in photoproduction at HERA*, *Eur. Phys. J.* **C 44** (2005) 351 [hep-ex/0508019] [INSPIRE].

[2] H1 collaboration, A. Aktas et al., *Inclusive production of D^+, D^0, D_s^+ and D^{*+} mesons in deep inelastic scattering at HERA*, *Eur. Phys. J.* **C 38** (2005) 447 [hep-ex/0408149] [INSPIRE].

[3] ZEUS collaboration, S. Chekanov et al., *Measurement of D mesons production in deep inelastic scattering at HERA*, *JHEP* **07** (2007) 074 [arXiv:0704.3562] [INSPIRE].

[4] ZEUS collaboration, H. Abramowicz et al., *Measurement of D^+ and Λ_c^+ production in deep inelastic scattering at HERA*, *JHEP* **11** (2010) 009 [arXiv:1007.1945] [INSPIRE].

[5] CLEO collaboration, D. Bortoletto et al., *Charm production in nonresonant e^+e^- annihilations at $\sqrt{s} = 10.55$ GeV*, *Phys. Rev.* **D 37** (1988) 1719 [*Erratum ibid.* **D 39** (1989) 1471] [INSPIRE].

[6] CLEO collaboration, P. Avery et al., *Inclusive production of the charmed baryon Λ_c from e^+e^- annihilations at $\sqrt{s} = 10.55$ GeV*, *Phys. Rev.* **D 43** (1991) 3599 [INSPIRE].

[7] ARGUS collaboration, H. Albrecht et al., *Observation of the charmed baryon Λ_c in e^+e^- annihilation at 10 GeV*, *Phys. Lett.* **B 207** (1988) 109 [INSPIRE].

[8] ARGUS collaboration, H. Albrecht et al., *Inclusive production of D^0, D^+ and $D^{*+}(2010)$ mesons in B decays and nonresonant e^+e^- annihilation at 10.6 GeV*, *Z. Phys.* **C 52** (1991) 353 [INSPIRE].

[9] ARGUS collaboration, H. Albrecht et al., *Production of D_s^+ mesons in B decays and determination of f_{D_s}*, *Z. Phys.* **C 54** (1992) 1 [INSPIRE].

[10] OPAL collaboration, G. Alexander et al., *A study of charm hadron production in $Z^0 \to c\bar{c}$ and $Z^0 \to b\bar{b}$ decays at LEP*, *Z. Phys.* **C 72** (1996) 1 [INSPIRE].

[11] OPAL collaboration, K. Ackerstaff et al., *Measurement of $f(c \to D^{*+}X)$, $f(b \to D^{*+}X)$ and $\Gamma(c\bar{c})/\Gamma_{\rm hadronic}$ using $D^{*\pm}$ mesons*, *Eur. Phys. J.* **C 1** (1998) 439 [hep-ex/9708021] [INSPIRE].

[12] ALEPH collaboration, R. Barate et al., *Study of charm production in Z decays*, *Eur. Phys. J.* **C 16** (2000) 597 [hep-ex/9909032] [INSPIRE].

[13] DELPHI collaboration, D. Bloch et al., *Measurement of the Z partial decay width into $c\bar{c}$ and multiplicity of charm quarks per b decay*, contributed paper to the *International Conference on High Energy Physics*, no. 122, Vancouver Canada July 22–29 1998 [DELPHI-98-120-CONF-181].

[14] LEP, ALEPH, DELPHI, L3, OPAL, LEP Electroweak Working Group, SLD Heavy Flavour and SLD Electroweak Groups collaborations, *A combination of preliminary electroweak measurements and constraints on the Standard Model*, CERN-EP-99-015 CERN, Geneva Switzerland (1999).

[15] DELPHI collaboration, P. Abreu et al., *Determination of $P(c \to D^{*+})$ and $BR(c \to \ell^+)$ at LEP-1*, *Eur. Phys. J.* **C 12** (2000) 209 [INSPIRE].

[16] L. Gladilin, *Charm hadron production fractions*, hep-ex/9912064 [INSPIRE].

JHEP09(2013)058

[17] ATLAS collaboration, *Measurement of $D^{(*)}$ meson production cross sections in pp collisions at $\sqrt{s} = 7$ TeV with the ATLAS detector*, ATLAS-CONF-2011-017, CERN, Geneva Switzerland (2011).

[18] ZEUS collaboration, U. Holm ed., *The ZEUS detector status report*, unpublished, available on http://www-zeus.desy.de/bluebook/bluebook.html, DESY, Germany (1993).

[19] N. Harnew et al., *Vertex triggering using time difference measurements in the ZEUS central tracking detector*, *Nucl. Instrum. Meth.* **A 279** (1989) 290 [INSPIRE].

[20] B. Foster et al., *The performance of the ZEUS central tracking detector z-by-timing electronics in a transputer based data acquisition system*, *Nucl. Phys. Proc. Suppl.* **B 32** (1993) 181.

[21] ZEUS collaboration, B. Foster et al., *The design and construction of the ZEUS central tracking detector*, *Nucl. Instrum. Meth.* **A 338** (1994) 254 [INSPIRE].

[22] ZEUS collaboration, A. Polini et al., *The design and performance of the ZEUS micro vertex detector*, *Nucl. Instrum. Meth.* **A 581** (2007) 656 [arXiv:0708.3011] [INSPIRE].

[23] M. Derrick et al., *Design and construction of the ZEUS barrel calorimeter*, *Nucl. Instrum. Meth.* **A 309** (1991) 77 [INSPIRE].

[24] ZEUS Calorimeter Group and ZEUS collaborations, A. Andresen et al., *Construction and beam test of the ZEUS forward and rear calorimeter*, *Nucl. Instrum. Meth.* **A 309** (1991) 101 [INSPIRE].

[25] A. Caldwell et al., *Design and implementation of a high precision readout system for the ZEUS calorimeter*, *Nucl. Instrum. Meth.* **A 321** (1992) 356 [INSPIRE].

[26] ZEUS Barrel Calorimeter Group collaboration, A. Bernstein et al., *Beam tests of the ZEUS barrel calorimeter*, *Nucl. Instrum. Meth.* **A 336** (1993) 23 [INSPIRE].

[27] J. Andruszków et al., *First measurement of HERA luminosity by ZEUS lumi monitor*, preprint DESY-92-066, DESY, Germany (1992).

[28] ZEUS collaboration, M. Derrick et al., *Measurement of total and partial photon proton cross-sections at* 180 *GeV center-of-mass energy*, *Z. Phys.* **C 63** (1994) 391 [INSPIRE].

[29] ZEUS Luminosity Group collaboration, J. Andruszkow et al., *Luminosity measurement in the ZEUS experiment*, *Acta Phys. Polon.* **B 32** (2001) 2025 [INSPIRE].

[30] M. Helbich et al., *The spectrometer system for measuring ZEUS luminosity at HERA*, *Nucl. Instrum. Meth.* **A 565** (2006) 572 [physics/0512153] [INSPIRE].

[31] T. Sjöstrand, S. Mrenna and P.Z. Skands, *PYTHIA* 6.4 *physics and manual*, *JHEP* **05** (2006) 026 [hep-ph/0603175] [INSPIRE].

[32] CTEQ collaboration, H. Lai et al., *Global QCD analysis of parton structure of the nucleon: CTEQ*5 *parton distributions*, *Eur. Phys. J.* **C 12** (2000) 375 [hep-ph/9903282] [INSPIRE].

[33] M. Glück, E. Reya and A. Vogt, *Photonic parton distributions*, *Phys. Rev.* **D 46** (1992) 1973 [INSPIRE].

[34] B. Andersson, G. Gustafson, G. Ingelman and T. Sjöstrand, *Parton fragmentation and string dynamics*, *Phys. Rept.* **97** (1983) 31 [INSPIRE].

[35] M. Bowler, *e^+e^- production of heavy quarks in the string model*, *Z. Phys.* **C 11** (1981) 169 [INSPIRE].

JHEP09(2013)058

[36] B. Andersson, G. Gustafson and B. Soderberg, *A general model for jet fragmentation*, *Z. Phys.* **C 20** (1983) 317 [INSPIRE].

[37] R. Brun et al., *Geant3*, technical report CERN-DD-EE-84-1, CERN, Geneva Switzerland (1987) [INSPIRE].

[38] W.H. Smith, K. Tokushuku and L.W. Wiggers, *The ZEUS trigger system*, in *Proc. Computing in High-Energy Physics (CHEP)*, Annecy France September 1992, C. Verkerk and W. Wojcik eds., CERN, Geneva Switzerland (1992), pg. 222 [DESY-92-150B].

[39] ZEUS collaboration, M. Derrick et al., *Observation of direct processes in photoproduction at HERA*, *Phys. Lett.* **B 322** (1994) 287 [INSPIRE].

[40] F. Jacquet and A. Blondel, *The kinematics of ep interactions*, in *Proceedings of the study for an ep facility in Europe*, U. Amaldi ed., Hamburg, Germany (1979), pg. 391 [DESY-79-048] [INSPIRE].

[41] G.M. Briskin, *Diffractive dissociation in ep deep inelastic scattering*, Ph.D. thesis, unpublished, Tel Aviv University, Tel Aviv Israel (1998) [INSPIRE].

[42] ZEUS collaboration, M. Derrick et al., *Study of $D^{*\pm}(2010)$ production in ep collisions at HERA*, *Phys. Lett.* **B 349** (1995) 225 [hep-ex/9502002] [INSPIRE].

[43] Particle Data Group collaboration, J. Beringer et al., *Review of particle physics (RPP)*, *Phys. Rev.* **D 86** (2012) 010001 [INSPIRE].

[44] ALEPH collaboration, D. Buskulic et al., *Charm counting in b decays*, *Phys. Lett.* **B 388** (1996) 648 [INSPIRE].

[45] OPAL collaboration, K. Ackerstaff et al., *Measurement of $f(c \to D^{*+}X)$, $f(b \to D^{*+}X)$ and $\Gamma(c\bar{c})/\Gamma_{\rm hadronic}$ using $D^{*\pm}$ mesons*, *Eur. Phys. J.* **C 1** (1998) 439 [hep-ex/9708021] [INSPIRE].

[46] ZEUS collaboration, H. Abramowicz et al., *Measurement of heavy-quark jet photoproduction at HERA*, *Eur. Phys. J.* **C 71** (2011) 1659 [arXiv:1104.5444] [INSPIRE].

[47] ZEUS collaboration, S. Chekanov et al., *Measurement of beauty photoproduction using decays into muons in dijet events at HERA*, *JHEP* **04** (2009) 133 [arXiv:0901.2226] [INSPIRE].

[48] ZEUS collaboration, S. Chekanov et al., *Beauty photoproduction using decays into electrons at HERA*, *Phys. Rev.* **D 78** (2008) 072001 [arXiv:0805.4390] [INSPIRE].

[49] OPAL collaboration, K. Ackerstaff et al., *Measurement of $f(c \to D^{*+}X)$, $f(b \to D^{*+}X)$ and $\Gamma(c\bar{c})/\Gamma_{\rm hadronic}$ using D*+- mesons*, *Eur. Phys. J.* **C 1** (1998) 439 [hep-ex/9708021] [INSPIRE].

[50] E. Lohrmann, *A summary of charm hadron production fractions*, arXiv:1112.3757 [INSPIRE].

[51] Particle Data Group collaboration, K. Nakamura et al., *Review of particle physics*, *J. Phys.* **G 37** (2010) 075021 [INSPIRE].

[52] Y.-J. Pei, *A simple approach to describe hadron production rates in e^+e^- annihilation*, *Z. Phys.* **C 72** (1996) 39 [INSPIRE].

[53] OPAL collaboration, R. Akers et al., *Inclusive strange vector and tensor meson production in hadronic Z^0 decays*, *Z. Phys.* **C 68** (1995) 1 [INSPIRE].

[54] DELPHI collaboration, P. Abreu et al., *Measurement of inclusive $K^{*0}(892)$, $\Phi(1020)$ and $K_2^{*0}(1430)$ production in hadronic Z decays*, *Z. Phys.* **C 73** (1996) 61 [INSPIRE].

JHEP09(2013)058

[55] K. Hamacher and M. Weierstall, *The next round of hadronic generator tuning heavily based on identified particle data*, hep-ex/9511011 [INSPIRE].

[56] ZEUS collaboration, S. Chekanov et al., *Measurement of K^0_S, Λ, $\bar{\Lambda}$ production at HERA*, *Eur. Phys. J.* **C 51** (2007) 1 [hep-ex/0612023] [INSPIRE].

[57] A. Ali and P. Söding eds., *High energy electron-positron physics*, in *Advanced series on directions in high energy physics*, vol. 1, Scientific Publishing Co., Singapore (1988),

JHEP09(2013)058

The ZEUS collaboration

H. Abramowicz[45,aj], I. Abt[35], L. Adamczyk[13], M. Adamus[54], R. Aggarwal[7,c], S. Antonelli[4], P. Antonioli[3], A. Antonov[33], M. Arneodo[50], O. Arslan[5], V. Aushev[26,27,aa], Y. Aushev,[27,aa,ab], O. Bachynska[15], A. Bamberger[19], A.N. Barakbaev[25], G. Barbagli[17], G. Bari[3], F. Barreiro[30], N. Bartosik[15], D. Bartsch[5], M. Basile[4], O. Behnke[15], J. Behr[15], U. Behrens[15], L. Bellagamba[3], A. Bertolin[39], S. Bhadra[57], M. Bindi[4], C. Blohm[15], V. Bokhonov[26,aa], T. Bołd[13], E.G. Boos[25], K. Borras[15], D. Boscherini[3], D. Bot[15], I. Brock[5], E. Brownson[56], R. Brugnera[40], N. Brümmer[37], A. Bruni[3], G. Bruni[3], B. Brzozowska[53], P.J. Bussey[20], B. Bylsma[37], A. Caldwell[35], M. Capua[8], R. Carlin[40], C.D. Catterall[57], S. Chekanov[1], J. Chwastowski[12,e], J. Ciborowski[53,an], R. Ciesielski[15,h], L. Cifarelli[4], F. Cindolo[3], A. Contin[4], A.M. Cooper-Sarkar[38], N. Coppola[15,i], M. Corradi[3], F. Corriveau[31], M. Costa[49], G. D'Agostini[43], F. Dal Corso[39], J. del Peso[30], R.K. Dementiev[34], S. De Pasquale[4,a], M. Derrick[1], R.C.E. Devenish[38], D. Dobur[19,u], B.A. Dolgoshein [33,†], G. Dolinska[15], A.T. Doyle[20], V. Drugakov[16], L.S. Durkin[37], S. Dusini[39], Y. Eisenberg[55], P.F. Ermolov [34,†], A. Eskreys [12,†], S. Fang[15,j], S. Fazio[8], J. Ferrando[20], M.I. Ferrero[49], J. Figiel[12], B. Foster[38,af], G. Gach[13], A. Galas[12], E. Gallo[17], A. Garfagnini[40], A. Geiser[15], I. Gialas[21,x], A. Gizhko[15], L.K. Gladilin[34], D. Gladkov[33], C. Glasman[30], O. Gogota[27], Yu.A. Golubkov[34], P. Göttlicher[15,k], I. Grabowska-Bołd[13], J. Grebenyuk[15], I. Gregor[15], G. Grigorescu[36], G. Grzelak[53], O. Gueta[45], M. Guzik[13], C. Gwenlan[38,ag], T. Haas[15], W. Hain[15], R. Hamatsu[48], J.C. Hart[44], H. Hartmann[5], G. Hartner[57], E. Hilger[5], D. Hochman[55], R. Hori[47], A. Hüttmann[15], Z.A. Ibrahim[10], Y. Iga[42], R. Ingbir[45], M. Ishitsuka[46], A. Iudin[27,ac], H.-P. Jakob[5], F. Januschek[15], T.W. Jones[52], M. Jüngst[5], I. Kadenko[27], B. Kahle[15], S. Kananov[45], T. Kanno[46], U. Karshon[55], F. Karstens[19,v], I.I. Katkov[15,l], M. Kaur[7], P. Kaur[7,c], A. Keramidas[36], L.A. Khein[34], J.Y. Kim[9], D. Kisielewska[13], S. Kitamura[48,al], R. Klanner[22], U. Klein[15,m], E. Koffeman[36], N. Kondrashova[27,ad], O. Kononenko[27], P. Kooijman[36], Ie. Korol[15], I.A. Korzhavina[34], A. Kotański[14,f], U. Kötz[15], N. Kovalchuk[27,ae], H. Kowalski[15], O. Kuprash[15], M. Kuze[46], A. Lee[37], B.B. Levchenko[34], A. Levy[45], V. Libov[15], S. Limentani[40], T.Y. Ling[37], M. Lisovyi[15], E. Lobodzinska[15], W. Lohmann[16], B. Löhr[15], E. Lohrmann[22], K.R. Long[23], A. Longhin[39,ah], D. Lontkovskyi[15], O.Yu. Lukina[34], J. Maeda[46,ak], S. Magill[1], I. Makarenko[15], J. Malka[15], R. Mankel[15], A. Margotti[3], G. Marini[43], J.F. Martin[51], A. Mastroberardino[8], M.C.K. Mattingly[2], I.-A. Melzer-Pellmann[15], S. Mergelmeyer[5], S. Miglioranzi[15,n], F. Mohamad Idris[10], V. Monaco[49], A. Montanari[15], J.D. Morris[6,b], K. Mujkic[15,o], B. Musgrave[1], V. Myronenko[27,ae], K. Nagano[24], T. Namsoo[15,p], R. Nania[3], A. Nigro[43], Y. Ning[11], T. Nobe[46], D. Notz[15], R.J. Nowak[53], A.E. Nuncio-Quiroz[5], B.Y. Oh[41], N. Okazaki[47], K. Olkiewicz[12], Yu. Onishchuk[27], K. Papageorgiu[21], A. Parenti[15], E. Paul[5], J.M. Pawlak[53], B. Pawlik[12], P. G. Pelfer[18], A. Pellegrino[36], W. Perlański[53,ao], H. Perrey[15], K. Piotrzkowski[29], P. Pluciński[54,ap], N.S. Pokrovskiy[25], A. Polini[3], A.S. Proskuryakov[34], M. Przybycień[13], A. Raval[15], D.D. Reeder[56], B. Reisert[35], Z. Ren[11], J. Repond[1], Y.D. Ri[48,am], A. Robertson[38], P. Roloff[15,n], I. Rubinsky[15], M. Ruspa[50], R. Sacchi[49], U. Samson[5], G. Sartorelli[4], A.A. Savin[56], D.H. Saxon[20], M. Schioppa[8], S. Schlenstedt[16], P. Schleper[22], W.B. Schmidke[35], U. Schneekloth[15], V. Schönberg[5], T. Schörner-Sadenius[15], J. Schwartz[31], F. Sciulli[11], L.M. Shcheglova[34], R. Shehzadi[5], R. Shevchenko[27,ab], S. Shimizu[47,n], O. Shkola[27,ae], I. Singh[7,c], I.O. Skillicorn[20], W. Słomiński[14,g], W.H. Smith[56], V. Sola[22], A. Solano[49], D. Son[28], V. Sosnovtsev[33], A. Spiridonov[15,q], H. Stadie[22], L. Stanco[39], N. Stefaniuk[27], A. Stern[45], T.P. Stewart[51], A. Stifutkin[33], P. Stopa[12], S. Suchkov[33], G. Susinno[8], L. Suszycki[13], J. Sztuk-Dambietz[22], D. Szuba[22], J. Szuba[15,r], A.D. Tapper[23], E. Tassi[8,d], J. Terrón[30], T. Theedt[15], H. Tiecke[36], K. Tokushuku[24,y], J. Tomaszewska[15,s], A. Trofymov[27,ae], V. Trusov[27], T. Tsurugai[32], M. Turcato[22], O. Turkot[27,ae,t], T. Tymieniecka[54], M. Vázquez[36,n], A. Verbytskyi[15], O. Viazlo[27], N.N. Vlasov[19,w], R. Walczak[38], W.A.T. Wan

JHEP09(2013)058

Abdullah[10], J.J. Whitmore[41,ai], K. Wichmann[15,t], L. Wiggers[36], M. Wing[52], M. Wlasenko[5], G. Wolf[15], H. Wolfe[56], K. Wrona[15], A.G. Yagües-Molina[15], S. Yamada[24], Y. Yamazaki[24,z], R. Yoshida[1], C. Youngman[15], N. Zakharchuk[27,ae], A.F. Żarnecki[53], L. Zawiejski[12], O. Zenaiev[15], W. Zeuner[15,n], B.O. Zhautykov[25], N. Zhmak[26,aa], A. Zichichi[4], Z. Zolkapli[10], D.S. Zotkin[34]

[1] *Argonne National Laboratory, Argonne, Illinois 60439-4815, U.S.A.* [A]
[2] *Andrews University, Berrien Springs, Michigan 49104-0380, U.S.A.*
[3] *INFN Bologna, Bologna, Italy* [B]
[4] *University and INFN Bologna, Bologna, Italy* [B]
[5] *Physikalisches Institut der Universität Bonn, Bonn, Germany* [C]
[6] *H.H. Wills Physics Laboratory, University of Bristol, Bristol, United Kingdom* [D]
[7] *Panjab University, Department of Physics, Chandigarh, India*
[8] *Calabria University, Physics Department and INFN, Cosenza, Italy* [B]
[9] *Institute for Universe and Elementary Particles, Chonnam National University, Kwangju, South Korea*
[10] *Jabatan Fizik, Universiti Malaya, 50603 Kuala Lumpur, Malaysia* [E]
[11] *Nevis Laboratories, Columbia University, Irvington on Hudson, New York 10027, U.S.A.* [F]
[12] *The Henryk Niewodniczanski Institute of Nuclear Physics, Polish Academy of Sciences, Krakow, Poland* [G]
[13] *AGH-University of Science and Technology, Faculty of Physics and Applied Computer Science, Krakow, Poland* [H]
[14] *Department of Physics, Jagellonian University, Cracow, Poland*
[15] *Deutsches Elektronen-Synchrotron DESY, Hamburg, Germany*
[16] *Deutsches Elektronen-Synchrotron DESY, Zeuthen, Germany*
[17] *INFN Florence, Florence, Italy* [B]
[18] *University and INFN Florence, Florence, Italy* [B]
[19] *Fakultät für Physik der Universität Freiburg i.Br., Freiburg i.Br., Germany*
[20] *School of Physics and Astronomy, University of Glasgow, Glasgow, United Kingdom* [D]
[21] *Department of Engineering in Management and Finance, Univ. of the Aegean, Chios, Greece*
[22] *Hamburg University, Institute of Experimental Physics, Hamburg, Germany* [I]
[23] *Imperial College London, High Energy Nuclear Physics Group, London, United Kingdom* [D]
[24] *Institute of Particle and Nuclear Studies, KEK, Tsukuba, Japan* [J]
[25] *Institute of Physics and Technology of Ministry of Education and Science of Kazakhstan, Almaty, Kazakhstan*
[26] *Institute for Nuclear Research, National Academy of Sciences, Kyiv, Ukraine*
[27] *Department of Nuclear Physics, National Taras Shevchenko University of Kyiv, Kyiv, Ukraine*
[28] *Kyungpook National University, Center for High Energy Physics, Daegu, South Korea* [K]
[29] *Institut de Physique Nucléaire, Université Catholique de Louvain, Louvain-la-Neuve, Belgium* [L]
[30] *Departamento de Física Teórica, Universidad Autónoma de Madrid, Madrid, Spain* [M]
[31] *Department of Physics, McGill University, Montréal, Québec, Canada H3A 2T8* [N]
[32] *Meiji Gakuin University, Faculty of General Education, Yokohama, Japan* [J]
[33] *Moscow Engineering Physics Institute, Moscow, Russia* [O]
[34] *Lomonosov Moscow State University, Skobeltsyn Institute of Nuclear Physics, Moscow, Russia* [P]
[35] *Max-Planck-Institut für Physik, München, Germany*
[36] *NIKHEF and University of Amsterdam, Amsterdam, Netherlands* [Q]
[37] *Physics Department, Ohio State University, Columbus, Ohio 43210, U.S.A.* [A]
[38] *Department of Physics, University of Oxford, Oxford, United Kingdom* [D]
[39] *INFN Padova, Padova, Italy* [B]
[40] *Dipartimento di Fisica dell' Università and INFN, Padova, Italy* [B]
[41] *Department of Physics, Pennsylvania State University, University Park, Pennsylvania 16802, U.S.A.* [F]

JHEP09(2013)058

[42] Polytechnic University, Tokyo, Japan [J]
[43] Dipartimento di Fisica, Università 'La Sapienza' and INFN, Rome, Italy [B]
[44] Rutherford Appleton Laboratory, Chilton, Didcot, Oxon, United Kingdom [D]
[45] Raymond and Beverly Sackler Faculty of Exact Sciences, School of Physics, Tel Aviv University, Tel Aviv, Israel [R]
[46] Department of Physics, Tokyo Institute of Technology, Tokyo, Japan [J]
[47] Department of Physics, University of Tokyo, Tokyo, Japan [J]
[48] Tokyo Metropolitan University, Department of Physics, Tokyo, Japan [J]
[49] Università di Torino and INFN, Torino, Italy [B]
[50] Università del Piemonte Orientale, Novara, and INFN, Torino, Italy [B]
[51] Department of Physics, University of Toronto, Toronto, Ontario, Canada M5S 1A7 [N]
[52] Physics and Astronomy Department, University College London, London, United Kingdom [D]
[53] Faculty of Physics, University of Warsaw, Warsaw, Poland
[54] National Centre for Nuclear Research, Warsaw, Poland
[55] Department of Particle Physics and Astrophysics, Weizmann Institute, Rehovot, Israel
[56] Department of Physics, University of Wisconsin, Madison, Wisconsin 53706, U.S.A. [A]
[57] Department of Physics, York University, Ontario, Canada M3J 1P3 [N]

[A] supported by the US Department of Energy
[B] supported by the Italian National Institute for Nuclear Physics (INFN)
[C] supported by the German Federal Ministry for Education and Research (BMBF), under contract No. 05 H09PDF
[D] supported by the Science and Technology Facilities Council, U.K.
[E] supported by HIR and UMRG grants from Universiti Malaya, and an ERGS grant from the Malaysian Ministry for Higher Education
[F] supported by the US National Science Foundation. Any opinion, findings and conclusions or recommendations expressed in this material are those of the authors and do not necessarily reflect the views of the National Science Foundation.
[G] supported by the Polish Ministry of Science and Higher Education as a scientific project No. DPN/N188/DESY/2009
[H] supported by the National Science Centre under contract No. DEC-2012/06/M/ST2/00428
[I] supported by the German Federal Ministry for Education and Research (BMBF), under contract No. 05h09GUF, and the SFB 676 of the Deutsche Forschungsgemeinschaft (DFG)
[J] supported by the Japanese Ministry of Education, Culture, Sports, Science and Technology (MEXT) and its grants for Scientific Research
[K] supported by the Korean Ministry of Education and Korea Science and Engineering Foundation
[L] supported by FNRS and its associated funds (IISN and FRIA) and by an Inter-University Attraction Poles Programme subsidised by the Belgian Federal Science Policy Office
[M] supported by the Spanish Ministry of Education and Science through funds provided by CICYT
[N] supported by the Natural Sciences and Engineering Research Council of Canada (NSERC)
[O] partially supported by the German Federal Ministry for Education and Research (BMBF)
[P] supported by RF Presidential grant N 3920.2012.2 for the Leading Scientific Schools and by the Russian Ministry of Education and Science through its grant for Scientific Research on High Energy Physics
[Q] supported by the Netherlands Foundation for Research on Matter (FOM)
[R] supported by the Israel Science Foundation

[a] now at University of Salerno, Italy
[b] now at Queen Mary University of London, United Kingdom
[c] also funded by Max Planck Institute for Physics, Munich, Germany
[d] also Senior Alexander von Humboldt Research Fellow at Hamburg University, Institute of Experimental Physics, Hamburg, Germany

JHEP09(2013)058

[e] also at Cracow University of Technology, Faculty of Physics, Mathematics and Applied Computer Science, Poland
[f] supported by the research grant No. 1 P03B 04529 (2005-2008)
[g] partially supported by the Polish National Science Centre projects DEC-2011/01/B/ST2/03643 and DEC-2011/03/B/ST2/00220
[h] now at Rockefeller University, New York, NY 10065, U.S.A.
[i] now at DESY group FS-CFEL-1
[j] now at Institute of High Energy Physics, Beijing, China
[k] now at DESY group FEB, Hamburg, Germany
[l] also at Moscow State University, Russia
[m] now at University of Liverpool, United Kingdom
[n] now at CERN, Geneva, Switzerland
[o] also affiliated with University College London, U.K.
[p] now at Goldman Sachs, London, U.K.
[q] also at Institute of Theoretical and Experimental Physics, Moscow, Russia
[r] also at FPACS, AGH-UST, Cracow, Poland
[s] partially supported by Warsaw University, Poland
[t] supported by the Alexander von Humboldt Foundation
[u] now at Istituto Nazionale di Fisica Nucleare (INFN), Pisa, Italy
[v] now at Haase Energie Technik AG, Neumünster, Germany
[w] now at Department of Physics, University of Bonn, Germany
[x] also affiliated with DESY, Germany
[y] also at University of Tokyo, Japan
[z] now at Kobe University, Japan
[†] deceased
[aa] supported by DESY, Germany
[ab] member of National Technical University of Ukraine, Kyiv Polytechnic Institute, Kyiv, Ukraine
[ac] member of National Technical University of Ukraine, Kyiv, Ukraine
[ad] now at DESY ATLAS group
[ae] member of National University of Kyiv - Mohyla Academy, Kyiv, Ukraine
[af] Alexander von Humboldt Professor; also at DESY and University of Oxford
[ag] STFC Advanced Fellow
[ah] now at LNF, Frascati, Italy
[ai] This material was based on work supported by the National Science Foundation, while working at the Foundation.
[aj] also at Max Planck Institute for Physics, Munich, Germany, External Scientific Member
[ak] now at Tokyo Metropolitan University, Japan
[al] now at Nihon Institute of Medical Science, Japan
[am] now at Osaka University, Osaka, Japan
[an] also at Łódź University, Poland
[ao] member of Łódź University, Poland
[ap] now at Department of Physics, Stockholm University, Stockholm, Sweden

JHEP09(2013)058